A NOVEL COLOR SPACE BASED ON RGB COLOR BARYCENTER

Qieshi Zhang †, *Sei-ichiro Kamata* ‡

† Information, Production and Systems Research Center, Waseda University, Japan
‡ Graduate School of Information, Production and Systems, Waseda University, Japan

ABSTRACT

Color space is one of the bases in the image processing area. Suitable color space can give the suitable description of colors for variant processing. However, in the image processing area, the existing color space cannot show the suitable distribution in color and lightness. In this paper, a novel color space based on RGB color barycenter (RGB-CB) is proposed to describe the color and lightness more intuitively. To prove the effectiveness of the proposed color space, YUV, HSV, $L^*a^*b^*$, and IPT color spaces are discussed and compared. Experimental results show the proposed color space can perform better effect than other color space in image processing.

***Index Terms*—** Color space, Color barycenter, Chroma, Saturation, Lightness

1. INTRODUCTION

The color space [1] is an abstract mathematical model, which gives a method or structure for color describing, classifying, comparing, and ordering. Based on the different property, the major color spaces can be divided into two categories. One is color mixture based, which mix all components to describe the colors. Such as RGB [2, 3, 4] color space. The other one is lightness-chroma based, which can separate color components into chroma and lightness respectively, such as YUV [5], $L^*a^*b^*$ [6], LUV [7], UVW [8], CIECAM02 [9, 10, 11] etc. color spaces. In the latter category, color spaces can be also divided into vision perception based model. HSV [12] is one of them and widely used in color analysis. Although the RGB, YUV, HSV, and $L^*a^*b^*$ color spaces are all applied in image processing, due to their definition and conversion, some problems still exist.

The purpose of this paper is to create a new color space which can be used to replace the applied color space to improve the effectiveness of existing image processing methods.

Problems in Chroma Representation: Although the existing color spaces are widely used in various applications, their capability in color representation is limited because their definitions. In this study, we will discuss the four famous color spaces: RGB, YUV, HSV, and $L^*a^*b^*$. For RGB color space, it difficult to describe the color intuitively because its mixture property. If we make change or design one color, we have to change the three color components respectively. For YUV and $L^*a^*b^*$ color spaces, the U-V and a^*-b^* color planes can reflect the chroma, but their color is deviated when the lightness is changed. In fact, the hue and saturation of color should be unchangeable. Therefore, these two color spaces are unsuitable for color analysis. To overcome above problems in image processing and satisfy the normal human visual system, the HSV color space is designed and be widely used to describe the color. However, the mapping function from RGB to HSV cannot keep the consistency of color intensity and vision perception. From the definition of saturation in HSV [12], we can find that when one or two components of RGB color space equal to zero, the saturation will equal to one. Therefore, it is incorrect to describe the color. In general, the existing color spaces cannot describe the chroma especially the intensity of color (saturation) precise and inconsistent with visual some times.

Problems in Lightness Representation: Besides, lightness representation of these color spaces also has some drawbacks in image processing. RGB color space cannot describe the lightness directly. Lightness of YUV and $L^*a^*b^*$ color spaces are inconsistent with chroma, because the weight of green is larger than blue. HSV color space only selects the max value of all color component as the lightness, so it cannot reflect the relation of chroma [12]. In general, the lightness component in the existing color spaces is inconsistent with the intensity of color. The weight of the conversion is fixed and only suitable for some colors, but other colors is unfair.

Based on the above discussions, we can conclude that the RGB color space is hard to analyze the color intuitively and cannot describe the lightness. YUV and $L^*a^*b^*$ color spaces are good at lightness representation and analysis, but they are hard to be used in color analysis. Although Lisper and Urban [13] modified the $L^*a^*b^*$ color space and obtain better color perception result, they didn't solve above problems. In addition, although HSV color space is intuitively and easy to be used in color processing, the saturation is inconsistent with vision and unsuitable for color analysis.

The contribution of this paper is proposing a novel color space which based on the color barycenter in RGB color space. Aiming at the shortcomings of existing color spaces which discussed above, proposed color space has better color and lightness representation ability and can be used simply.

978-1-4799-9988-0/16/$31.00 ©2016 IEEE

2. PROPOSED NEW COLOR SPACE

2.1. RGB Color Barycenter (RGB-CB)

In our previous work [14], the unformed RGB-CB is proposed and used in road-sign detection [15, 16]. To obtain the RGB-CB, the RGB color triangle (RGB-CT) is converted from RGB cube and used to calculate the corresponding RGB-CB. RGB-CB is the barycenter of (R, G, B) in RGB color space. However, if we calculate it directly, the barycenters distribution will show as a small cube which has similar properties as RGB color space. For calculating the RGB-CB more reasonable and reflecting more properties of color distribution, RGB-CT is presented and described as flows:

Firstly, as Fig. 1 shown, to create the RGB-CT, all color (R, G, B) in 3D RGB color cube (Fig. 1(a)) are projected onto 2D plane (Fig. 1(b)). The star mark ($'\star'$) in the Fig. 1(a) is a color in the RGB color cube (one point in 3D space). For this point (pixel), its corresponding RGB-CT can be created:

1. Represent three components (R, G, B) of a color in RGB color space as three vectors (R', G', B').
2. Project the vectors (R', G', B') onto the 2D plane with $2\pi/3$ angle, as shown in Fig.1(b). The modules of the three vectors are limited to [0, 255], because the values of R_v, G_v, and B_v components are in this range.
3. Connect the three apexes of the vectors to create the color triangle as the triangle shown in Fig.1(b).

By this conversion, different colors will project into different color triangles. The full distribution of RGB-CD is shown as hexagon region (Fig. 2). For pure colors, the RGB-CTs are lines. For gray levels, the color triangles are equilateral triangles. For the other colors in RGB color space, the (R, G, B) values are various and their RGB-CTs are changeable. From these instances, we can conclude that the position of RGB-CB is corresponding to the shape of RGB-CT, also can be used to describe the intensity and angle degree of color. Therefore, based on the RGB-CT, the corresponding RGB-CB can be computed to reflect the color feature.

Secondly, in order to calculate the RGB-CB from RGB-CT easily, the apexes of RGB-CT are defined as (R_x, R_y), (G_x, G_y), and (B_x, B_y) in 2D rectangle coordinate system as shown in Fig. 2 by Eq. (1):

$$\begin{cases} (R_x, R_y) = (0, R) \\ (G_x, G_y) = \left(-\frac{\sqrt{3}}{2}G, -\frac{1}{2}G\right) \\ (B_x, B_y) = \left(\frac{\sqrt{3}}{2}B, -\frac{1}{2}B\right) \end{cases}, \tag{1}$$

where the R, G, and B are original values of color in RGB color space. The rectangle coordinates of RGB-CB (C_x, C_y) can be calculated by Eq. (2):

$$\begin{cases} C_x = \frac{1}{3}(R_x + G_x + B_x) = \left(0 - \frac{\sqrt{3}}{6}G + \frac{\sqrt{3}}{6}B\right) \\ C_y = \frac{1}{3}(R_y + G_y + B_y) = \left(\frac{1}{3}R - \frac{1}{6}G - \frac{1}{6}B\right) \end{cases} \tag{2}$$

2.2. New Color Space

Similar as the existing color space, the proposed color space also 3D and each point is defined by three unique color components: hue (C_φ), saturation (C_r), and lightness (C_z). The axes and arrangement of colors to define the perceptual of the space. These color components are defined as follows:

$$C_\varphi = \begin{cases} 0, & B–G{=}0, 2R–G–B{=}0 \\ \arctan\left(\frac{2R–G–B}{-\sqrt{3}G+\sqrt{3}B}\right), & B–G{>}0, 2R–G–B{\geq}0 \\ \pi/2, & B–G{=}0, 2R–G–B{>}0 \\ \arctan\left(\frac{2R–G–B}{-\sqrt{3}G+\sqrt{3}B}\right)+\pi, & B–G{<}0 \\ 3\pi/2, & B–G{=}0, 2R–G–B{<}0 \\ \arctan\left(\frac{2R–G–B}{-\sqrt{3}G+\sqrt{3}B}\right)+2\pi, & B–G{>}0, 2R–G–B{\leq}0 \end{cases} \tag{3}$$

$$C_r = \frac{1}{3}\sqrt{[R^2 + G^2 + B^2 - (RG + RB + BG)]}, \tag{4}$$

$$C_z = \omega_{CR} \cdot R + \omega_{CG} \cdot G + \omega_{CB} \cdot B, \tag{5}$$

where ω_{CR}, ω_{CG}, and ω_{CB} are the weights of the lightness conversion, which will be discussed later. Based on above equations, the RGB color space can be converted to a new color space as shown in Fig. 3.

In the above equations, the hue (C_φ) and saturation (C_r) are calculated from the Eq. (2) directly by the coordinate conversion as follows:

$$C\varphi = \begin{cases} 0, & C_x = 0,\ C_y = 0 \\ \texttt{arctan}(C_y/C_x), & C_x > 0,\ C_y \geq 0 \\ \pi/2, & C_x = 0,\ C_y > 0 \\ \texttt{arctan}(C_y/C_x) + \pi, & C_x < 0 \\ 3\pi/2, & C_x = 0,\ C_y < 0 \\ \texttt{arctan}(C_y/C_x) + 2\pi, & C_x\ 0,\ C_y \leq 0 \end{cases} \tag{6}$$

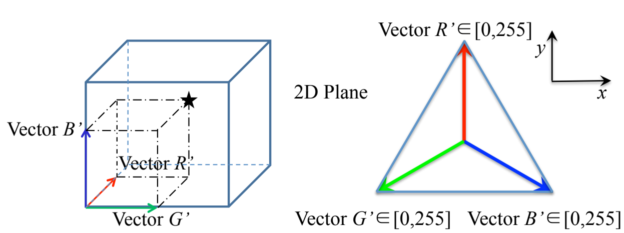

(a) RGB color space (b) Color Triangle

Fig. 1. Creation of RGB Color Triangle (RGB-CT).

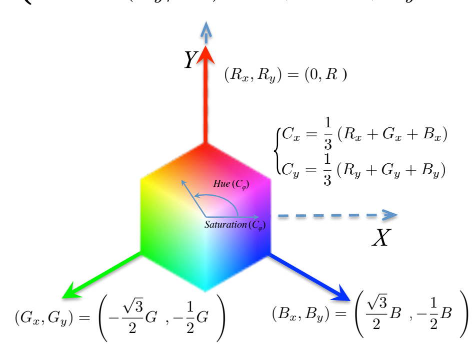

Fig. 2. Full distribution of RGB-CB.

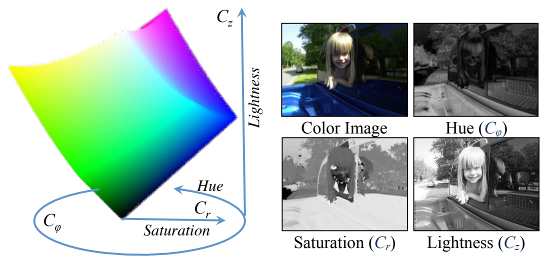

(a) $C_\varphi C_r C_z$ Color Space (b) Example

Fig. 3. $C_\varphi C_r C_z$ Color Space.

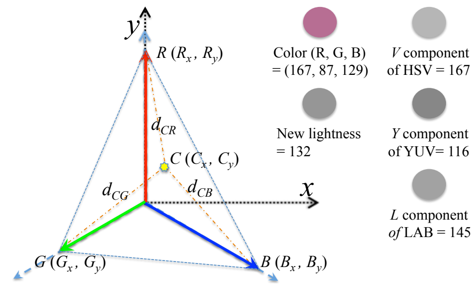

Fig. 4. Distances from RGB-CB to Apexes of RGB-CT.

$$Cr = \sqrt{C_x^2 + C_y^2} \tag{7}$$

where $C_\varphi \in (0, 2\pi]$, $C_r \in [0, 85]$ based on the definition of the RGB-CT. C_φ can be used to describe hue, and C_r can be used to describe saturation. Also, the distribution of C_φ and C_r can be used to describe the color for different purpose. And show better description ability than HSV color space which discussed in the experiment part.

For the definition of lightness (C_z), it is different from the existing color space. The proposed lightness component takes the relationship of R, G, and B components into account, and the weights of R, G, and B components are adaptively determined during creation. Here, the distances from the RGB-CB to the apexes of RGB-CT are set as d_{CR}, d_{CG}, and d_{CB}, respectively, as shown in Fig 4. Normalize them as the weights:

$$\begin{cases} \omega_{CR} = d_{CR}/(d_{CR} + d_{CG} + d_{CB} + C_0) \\ \omega_{CG} = d_{CG}/(d_{CR} + d_{CG} + d_{CB} + C_0) \\ \omega_{CB} = d_{CB}/(d_{CR} + d_{CG} + d_{CB} + C_0) \end{cases}, \tag{8}$$

where C_0 is constant (in this paper C_0 set as 0.0001 simply), d_{CR}, d_{CG}, and d_{CB} are defined as:

$$\begin{cases} d_{CR} = \sqrt{(C_x - R_x)^2 + (C_y - R_y)^2} \\ d_{CG} = \sqrt{(C_x - G_x)^2 + (C_y - G_y)^2} \\ d_{CB} = \sqrt{(C_x - B_x)^2 + (C_y - B_y)^2} \end{cases}, \tag{9}$$

2.3. Characteristic of Proposed Color Space

As the Fig. 3 shown, the proposed color space can be used to describe the chrome (hue and saturation) and lightness which similar as HSV color space. Although the meaning of all components in the proposed color space is similar to HSV, the definitions are different which discussed above.

2.3.1. Chrome Representation

For the gray level colors, their barycenters are at the same point (the origin point) because the shapes of their color triangles are all equilateral triangles. In this situation, the offset of barycenter is 0, it is corresponding to the feature of gray (no color information). For other colors, one color (R, G, B) only has one unique barycenter. The offset of RGB-CB from the original point of RGB-CT can be used to reflect the color feature and all the possible points are distributed in a hexagon region as shown in Fig. 2. Different position means different color and these colors can be classified into seven regions, namely, magenta, red, yellow, green, cyan, blue, and luminance. Based on this property, the C_φ and C_r components can be used to instead of H and S components in HSV.

2.3.2. Lightness Representation

Due to the lightness of the proposed color space is based on the intensity of color, therefore it can perform different lightness from other color spaces as shown in Fig. 4. The advantage of the proposed color space will be discussed and compared with other four widely used color space.

3. EXPERIMENTAL RESULTS

Due to the main contribution of this paper is proposing a new color space, so the widely used color space, such as RGB, YUV, HSV, $L^*a^*b^*$, and IPT [17] are compared. To evaluate the advantage of the proposed color space, the chroma and lightness representation ability and color similarity measure are compared. To compare the computation time with each color space, three largest public databases are used: LIVE [18], CSIQ [19], and TID2008 [20]. Fig. 5 shows the computation time under Matlab 2010 in our PC. Although the result shows that the proposed method not faster than YUV and HSV color spaces, it also can be used in real-time.

3.1. Advantage in Chroma Presentation

Generally, if the saturation can amplify the details and accord with visual experience, it will facilitates in color separation. If one or two component of RGB color space equal to 0, the value of saturation in HSV is incorrect for describing the intensity of color. Fig. 6 gives an example to compare the

	YUV	HSV	RGB-CB	IPT	L^*a^*b
LIVE	14ms	40ms	53ms	148ms	171ms
CSIQ	7ms	28ms	39ms	106ms	121ms
TID2008	6ms	19ms	28ms	82ms	96ms

Fig. 5. Average Computation Time.

Table 1. Comparison of Lightness Representation.

	Quality Aware Clustering (QAC)					Image Entropy (IE)					Anisotropic Quality Index (AQI)				
	RGB-CB	YUV	HSV	$L^*a^*b^*$	IPT	RGB-CB	YUV	HSV	$L^*a^*b^*$	IPT	RGB-CB	YUV	HSV	$L^*a^*b^*$	IPT
LIVE	**0.755**	0.751	0.746	0.755	**0.756**	**7.353**	7.331	7.297	6.922	7.290	**2.951**	**3.004**	2.615	0.772	2.496
CSIQ	**0.739**	0.739	0.739	0.732	**0.749**	**7.244**	7.251	**7.278**	6.986	7.249	**3.550**	**3.748**	3.241	1.912	2.823
TID2008	**0.751**	0.747	0.731	0.743	**0.753**	**7.165**	7.128	7.101	6.769	7.097	**2.799**	**2.819**	2.445	0.766	2.324

RGB-CB HSV RGB-CB HSV

(a) Color image (b) Hue Component (c) Saturation Component

Fig. 6. Intuitive Comparison with RGB-CB and HSV.

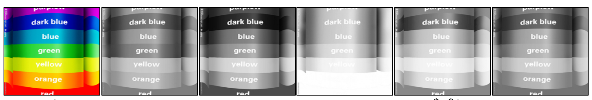

Color RGB-CB YUV HSV L^*a^*b IPT

Fig. 7. Example of Lightness in Different Color Space.

proposed color space and HSV color space in hue and saturation components. As this example shown, the main difference in hue (Fig. 6(b)) is that the degree of hue shifts 90 degrees, in the proposed RGB-CB the minimum (0°) and maximum (360°) values are magenta, but in HSV is red. Theoretically, the shifted degree doesn't influence the color to distinguish ability. But the human visual is more sensitive in red than magenta, this is why in Fig. 6(b) the RGB-CB has better visual effect than HSV color space. Different from hue, the comparison of saturation in Fig. 6(c) shows that the proposed color barycenter can perform better vision effect and consistent with human vision than HSV. Compared with Fig. 6(c), in the dark color region, the saturation in HSV color space has large values (appears bright), such as the background region of the face. In the bright color region, the saturation of HSV color space is small (appears as dark), such as the cheek region of the face. It is strange for observation and color analysis. Different from HSV color space, our color space can obtain acceptable results which are consistent with vision.

3.2. Advantage in Lightness Presentation

To compare these color spaces objective, three no-reference quality assessment evaluations are used: Quality Aware Clustering (QAC) [21], Image Entropy (IE), and Anisotropic Quality Index (AQI) [22]. Table 1 shows the comparison among QAC, IE, and AQI in LIVE [18], CSIQ [19], and TID2008 [20] databases. For QAC, proposed color space can obtain the higher score than other spaces expect the IPT which only a little lower than it. For IE, only in CSIQ database the score of the proposed color space is little lower than YUV and HSV. For AQI, although proposed color space is lower than YUV, it is much better than other color spaces.

In general, the proposed color space has better lightness presentation ability than HSV, and better or close effect to YUV, $L^*a^*b^*$, and IPT color spaces in most situations. This means, for most color-to-gray based processing, the RGB-CB can support better input lightness image than others. For observing the difference between color spaces in view, Fig. 7 gives an example for comparison. From this example, we can see that the HSV color space cannot show the color difference in lightness component, and $L^*a^*b^*$ looks no good than other color spaces.

Table 2. Color Similarity Measure Ability Comparison.

Color Space / Database	Color Cluster by K-means (K=7) with PSNR				
	RGB	RGB-CB	YUV	HSV	$L^*a^*b^*$
LIVE	32.69	**33.17**	31.49	30.61	32.09
CSIQ	32.05	**32.33**	30.59	29.32	31.84
TID2008	32.55	**32.48**	32.08	29.60	31.93

3.3. Advantage of RGB-CB in Color Similarity Measure

Besides the lightness comparison, the color description ability of combined components also be compared with the K-means [23] color reduction in different color spaces. Table 2 gives the PSNR in the different color space. In this example, K-means based color reduction is applied to compare the ability of color similarity measure between proposed RGB-CB based color space and other color spaces. From this example, the proposed color space can obtain a higher PSNR than other color space which includes the original RGB color space. It shows that the proposed color space has higher color similarity measure ability.

3.4. Application Area

The proposed color space already be tested in some applications and obtain better or similar results which compared with HSV color space, such as classification [24], face detection [25], road sign detection [26], contract enhancement [27], haze removal [28] etc.

4. CONCLUSIONS

In this paper, a novel color space based on RGB color barycenter is proposed. The experimental results showed that the proposed color space has better chroma and lightness representation. In our research and testing, the proposed color space can replace the HSV in the image processing area directly. The future work is using it in the different research topic to test the performance.

5. REFERENCES

[1] R.G. Kuehni, "Color space and its divisions," *1st ed. New York: Wiley*, 2003.

[2] "A standard default color space for the Internet," http://www.w3.org/Graphics/Color/sRGB.html.

[3] "scRGB," http://www.color.org/chardata/rgb/scrgb.xalter.

[4] "Adobe RGB (1998) color image encoding," http://www.adobe.com/digitalimag/adobergb.html.

[5] "YUV Color Space," http://en.wikipedia.org/wiki/YUV.

[6] Gernot Hoffmann, "CIE Lab color space," http://www.color.org/ROMMRGB.pdf.

[7] "CIE LUV," http://en.wikipedia.org/wiki/CIELUV.

[8] "CIE UVW," http://en.wikipedia.org/wiki/CIE1964.

[9] Nathan Moroney, Mark D. Fairchild, Robert W.G. Hunt, Changjun Li, M. Ronnier Luo, and Todd Newman, "The CIECAM02 color appearance model," *Tenth Color Imaging Conference*, Nov. 2002.

[10] Fairchild and D. Mark, "Color appearance models: CIECAM02 and beyond," *12th Color Imaging Conference*, Nov. 2004.

[11] CIE, "A color appearance model for color management systems: CIECAM02," *Technical Report*, vol. 89, 2004.

[12] G.H. Joblove and D. Greenberg, "Color spaces for computer graphics," *Computer Graphics*, vol. 12, no. 3, pp. 20–25, Aug. 1978.

[13] I. Lissner and P. Urban, "Toward a unified color space for perception-based image processing," *IEEE Trans. on Image Processing*, vol. 21, no. 3, pp. 1153–1168, 2012.

[14] Q. Zhang and S. Kamata, "Automatic road sign detection method based on color barycenters hexagon model," *Int'l Conf. on Pattern Recognition (ICPR)*, pp. 1–4, 2008.

[15] Q. Zhang and S. Kamata, "A novel color descriptor for road-sign detection," *IEICE Trans. on Fundamentals of Electronics, Communications and Computer Sciences*, vol. E96-A, no. 5, pp. 971–979, May 2013.

[16] Q. Zhang and S. Kamata, "Improved color barycenter model and its separation for road sign detection," *IEICE Trans. on Information and Systems*, vol. E96-D, no. 12, pp. 2839–2849, Dec. 2013.

[17] F. Ebner, Fairchild, and D. Mark, "Development and testing of a color space (IPT) with improved hue uniformity," *Color and Imaging Conference*, , no. 1, pp. 8–13, 1998.

[18] H. Sheikh, Z. Wang, L. Cormack, and A. Bovik, "Live image quality assessment database release 2," 2005.

[19] E. Larson and D. Chandler, "Most apparent distortion: fullreference image quality assessment and the role of strategy," *J. of Electronic Imaging*, vol. 19, no. 1, pp. 011006, 2010.

[20] N. Ponomarenko, V. Lukin, A. Zelensky, K. Egiazarian, M. Carli, and F. Battisti, "Tid2008-a database for evaluation of full-reference visual quality assessment metrics," *Advances of Modern Radioelectronics*, vol. 10, no. 10, pp. 30–45, 2009.

[21] W. Xue, L. Zhang, and X. Mou, "Learning without human scores for blind image quality assessment," *Proc. of IEEE Conf. on Computer Vision and Pattern Recognition (CVPR)*, pp. 995–1002, 2013.

[22] S. Gabarda and G. Cristobal, "Blind image quality assessment through anisotropy," *J. Optical Society of America*, vol. 24, no. 12, pp. B42–B51, Dec. 2007.

[23] T. Kanungo, D.M. Mount, N.S. Netanyahu, C.D. Piatko, R. Silverman, and A.Y. Wu, "An efficient k-means clustering algorithm: Analysis and implementation," *IEEE Trans. on Pattern Recognition and Machine Intelligence (PAMI)*, vol. 24, no. 7, pp. 881–892, 2002.

[24] S. Ni, Q. Zhang, S. Kamata, and C. Zhang, "Learning discriminative and shareable patches for scene classification," *IEEE Int'l Conf. on Acoustics, Speech and Signal Processing (ICASSP)*, 2016.

[25] Q. Zhang, S. Kamata, and J. Zhang, "Face detection and tracking in color images using color centroids segmentation," *IEEE Int'l Conf. on Robotics and Biomimetics (ROBIO)*, pp. 1008–1013, 2008.

[26] Q. Zhang, S. Kamata, and J. Zhang, "Color barycenter hexagon model based road sign detection," *Int'l Multi-Conf. of Engineers and Computer Scientists (IMECS*, vol. 1, pp. 667–670, 2008.

[27] Q. Zhang, H. Inaba, and S. Kamata, "Adaptive histogram analysis for image enhancement," *Pacific-Rim Symp. on Image and Video Technology (PSIVT)*, pp. 408–413, 2010.

[28] Q. Zhang and S. Kamata, "Improved optical model based on region segmentation for single image haze removal," *Int'l J. of Information and Electronics Engineering (IJIEE)*, vol. 2, no. 1, pp. 62–68, 2012.